

MedChemComm

Accepted Manuscript



This is an *Accepted Manuscript*, which has been through the Royal Society of Chemistry peer review process and has been accepted for publication.

Accepted Manuscripts are published online shortly after acceptance, before technical editing, formatting and proof reading. Using this free service, authors can make their results available to the community, in citable form, before we publish the edited article. We will replace this *Accepted Manuscript* with the edited and formatted *Advance Article* as soon as it is available.

You can find more information about *Accepted Manuscripts* in the [Information for Authors](#).

Please note that technical editing may introduce minor changes to the text and/or graphics, which may alter content. The journal's standard [Terms & Conditions](#) and the [Ethical guidelines](#) still apply. In no event shall the Royal Society of Chemistry be held responsible for any errors or omissions in this *Accepted Manuscript* or any consequences arising from the use of any information it contains.

Virtual screening for novel Atg5-Atg16 complex inhibitors for autophagy modulation

*Elizabeth Robinson¹, Euphemia Leung², Anna M. Matuszek³, Niels Krosggaard-Larsen³, Daniel P. Furkert³, Margaret A. Brimble³, Alan Richardson¹ and Jóhannes Reynisson^{*3}*

¹ Institute for Science and Technology in Medicine, Keele University, Guy Hilton Research Centre, Stoke-on-Trent, United Kingdom

² Auckland Cancer Society Research Centre, The University of Auckland, New Zealand

³ School of Chemical Sciences, The University of Auckland, New Zealand

*To whom correspondence should be addressed: School of Chemical Sciences, The University of Auckland, Private Bag 92019, Auckland 1142, New Zealand.
E-mail: j.reynisson@auckland.ac.nz, Tel. 64-9-373-7599 ext. 83746, Fax. 64-9-373-7422

Abstract

Two hit compounds (**14** and **62**) were identified using virtual high throughput screening (vHTS) inhibiting the autophagy process in A2780 ovarian cancer cells. The expression levels of the LC3-II and p62 autophagy marker proteins were monitored using Western blotting. Preliminary structure activity relationship (SAR) study of close structural analogues revealed another active compound **38**. The three active compounds were tested in the MCF-7 human breast cancer cells and severe reduction of autophagosomes formation was observed confirming the activity of the inhibitors. The docking scaffold used for the vHTS was a lipophilic cleft on the Atg5 protein, which is occupied by a phenylalanine residue in the Atg16 polypeptide. To the best of our knowledge this is the first report on inhibitors that specifically modulate autophagy by directly inhibiting autophagy specific proteins, which is significant due the role autophagy plays in a number of morbid diseases such as cancer.

Introduction

Autophagy (self-eating) is a catabolic pathway that sequesters undesired cellular material into autophagosomes for delivery to lysosomes for the bulk degradation and is conserved in most eukaryotes.¹ Autophagic dysfunction is now associated with a number of diseases, including infection by pathogens, inflammatory bowel disease, neurodegeneration and cancer.²⁻⁴ A number of small molecules are known to modulate autophagy however there is a dearth of compounds that directly interact with the specific autophagy proteins.⁵ A key step in the pathway is the covalent conjugation of the ubiquitin-related protein Atg8 (autophagy) to phosphatidylethanolamine in autophagic membranes by a complex consisting of Atg16 and the Atg12–Atg5 conjugate.¹ The crystal structure of the Atg5–Atg16 complex is known and *in vitro* analysis showed that the Arg-35 and Phe-46 amino acids of Atg-16 are crucial for this interaction to take place.^{6, 7} The binding pockets are shown in Figure 1. This protein complex therefore represents a new target for drug development,⁸ in particular for a virtual high throughput screening (vHTS) campaign, which is an effective method to generate inhibitors of bio-molecular targets.⁹⁻¹¹

In this study, the crystal structure of the Atg5–Atg16 complex at the binding site of Phe-46 in Atg-16 was used as a docking scaffold for a vHTS to find small molecular inhibitors for the autophagy process in ovarian and breast cancer cell lines.

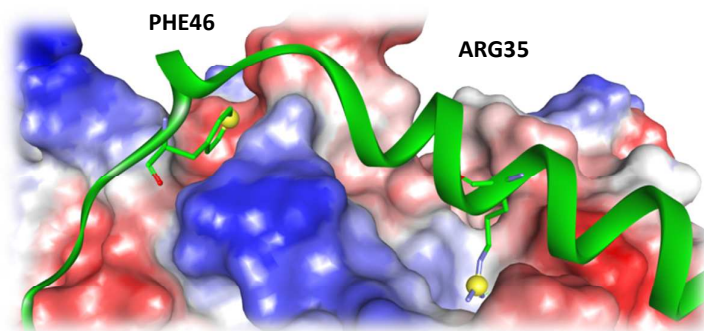


Figure 1. The two binding pockets of interest of the Atg5–Atg16 complex identified by mutation studies. The Atg5 protein surface is rendered and the Atg16 polypeptide is green. The amino acids Arg35 and Phe46 are shown in the stick format.

Results

Pilot screen

1×10^4 molecular entities were downloaded from the ChemBridge diversity collection.¹² It was filtered to render the list Lipinski¹³ compliant, resulting in 8373 molecules. These were screened against the cleft in Atg5 which the phenyl moiety of Phe-46 from the Atg16 polypeptide occupies. The binding pocket at Arg-35 (see Figure 1) was also considered but several amino acids were missing from the crystal structure, which are a part of a flexible loop directly in this pocket. The proximity of the loop makes the shape of the pocket uncertain and less attractive as a docking scaffold than the cleft for Phe-46 and it was therefore not considered further. The GoldScore¹⁴ and ChemScore^{15, 16} fitness functions were used for the initial screen. All ligands without predicted hydrogen bonding were eliminated as well as those with low ChemScore (<10); no such low values were predicted by GoldScore. This left 512 candidates, which were screened again with high search efficiency using both scoring functions. The candidates were eliminated based on the GoldScore (≤ 30) and ChemScore (≤ 20); and the ability to form hydrogen bonds based on both scoring functions resulting in 33 candidates. The results were inspected visually for consensus of the best predicted configuration of the ligands between the scoring functions, that the ligands had

plausible configurations, *i.e.*, not strained, for lipophilic moieties pointing into the water environment and, finally for undesirable moieties linked to cell toxicity and chemical reactivity.¹⁷ The screening methodology used has been previously successfully applied to find active ligands of the phosphoinositide specific-phospholipase C- γ 2 enzyme.¹⁸ Eighteen compounds were selected for experimental testing and their structures are shown in Table 1. A detailed description of the vHTS is given in the Methodology section.

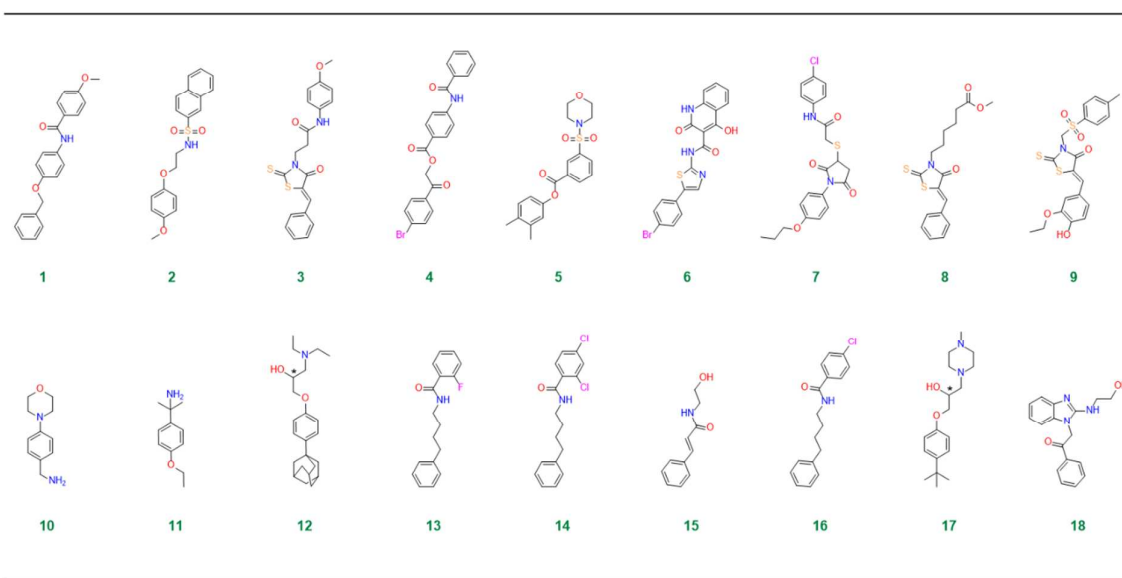


Table 1. The structures of the eighteen compounds experimentally tested for autophagy activity. Compounds **12** and **17** were tested as the racemates.

Biological testing

Microtubule-associated protein light chain 3 (LC3-II) is the mammalian ortholog of yeast Atg-8 and a robust marker of autophagosomes.¹⁹ LC3 binds the polyubiquitin-binding protein p62, an adapter protein that is selectively degraded via autophagy.⁸ The eighteen virtual hits were tested in A2780 ovarian tumour cell line for efficacy. Autophagy was induced by starvation (PBS buffer for 3 hours) and the effect of the ligands was assessed by measuring accumulation of LC3-II and p62 by immunoblotting (see methodology for detailed description). A decrease in LC3-II and increase in p62 is consistent with suppression of autophagy. Two set of experiments were conducted for each compound. The representative

results are shown in Figure 2 for compounds **10** - **18** and in Figure S1 in the Supplementary Information for compounds **1** - **9**; quantitation of both sets of data is also provided in the Supplementary Information (Fig. S6 and S7).

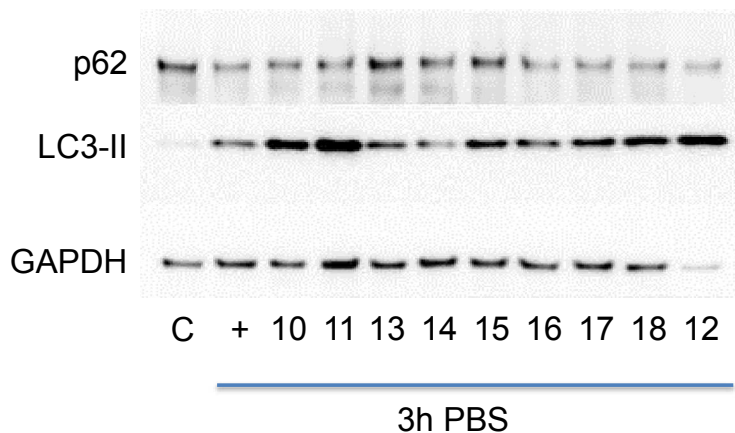


Figure 2. Immunoblotting of p62 and LC3-II protein in ovarian cancer A2780 cell line. Cells were incubated with DMSO as negative control (C), or PBS for 3 h to induce autophagy without (+) or with pre-incubation of compounds for 1 h. p62 and LC3-II were detected in total cell extracts by western blotting analysis, using specific antibodies. GAPDH (Glyceraldehyde 3-phosphate dehydrogenase) was used as loading control. The quantitative results are given in Fig. S7 in the Supplementary.

The control profile of the cellular proteins as base line was shown on the left lane in Figure 2. Upon induction of autophagy, the expected decrease in LC3-II and increase in p62 was observed. Compounds **13** and **14** reduced accumulation of LC3-II and depletion of p62. Dose response experiments were performed to verify this activity of these ligands (Figures S2 and S3 in the Supplementary Information section). These experiments demonstrated the activity of compound **14** was dose dependant (Figure 3), but this was not apparent for ligand **13**.

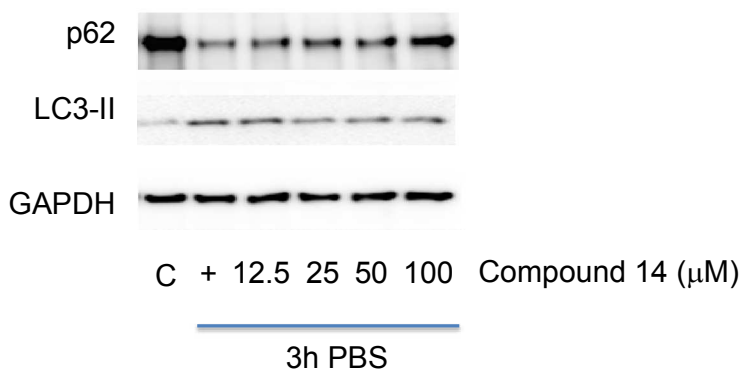
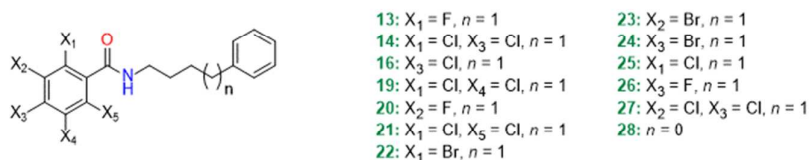


Figure 3. Dose response effect for ligand **14** using immunoblotting of p62 and LC3-II protein in ovarian cancer A2780 cell line. Cells were incubated with DMSO as negative control (C), or PBS for 3 h to induce autophagy (+) without or with pre-incubation of indicated concentration of compound **14** for 1 h. GAPDH was used as loading control. The quantitative result for compound **14** is given in Fig. S8 in the Supplementary Information.

It can be clearly seen in Figure 3 that an increased concentration of ligand **14** causes the re-emergence of p62 compared to the second lane (+) of autophagy cells and the reduction of LC3-II, which is a strong indication that the ovarian cell are reverted from their autophagy state.

Preliminary Structural Activity Relationship (SAR)

In order to explore the chemical space around the hit compound **14** ten close structural analogues were purchased and tested. In addition two compounds (**13** and **16**) from the pilot screen are similar to **14** resulting in thirteen molecules for the SAR analysis (Scheme 1).



Scheme 1. The structures of twelve close structural analogues of hit compound **14**, which were tested for their activity for SAR generation.

Various single and double chlorine substitutions of the benzamide ring did *not* lead to active compounds suggesting that the *ortho* / *para* substitution pattern is crucial for the efficacy observed. *Ortho* and *para* fluorine single substitutions (**13** and **26**) on the benzamide ring were not tolerated. Furthermore, bromine single substitution (*ortho* (**22**), *meta* (**23**) and *para* (**24**)) gave inconsistent effects on the expression levels of LC3-II and p62. There is not a clear indication of inhibition and it can be concluded that single bromine substitution of the benzamide ring is not favourable. Finally, one derivative (**28**) with a shorter aliphatic chain ($n = 0$) and no substitution on the ring systems was not active. In conclusion, the *ortho* / *para* chlorine substitution pattern is vital for the activity. Three compounds, **29** – **31**, with the *ortho* / *para* chlorine substitution on the benzamide were tested and their structures are shown in Table 2. None of the ligands demonstrated consistent activity, which suggests that the dichlorinated benzamide moiety is on its own insufficient to modulate Autophagy.

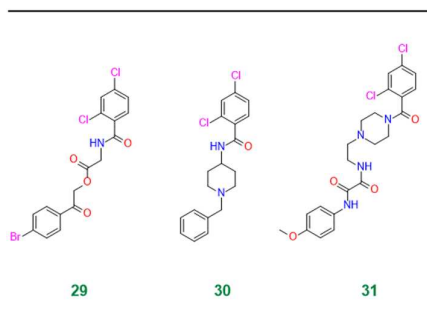
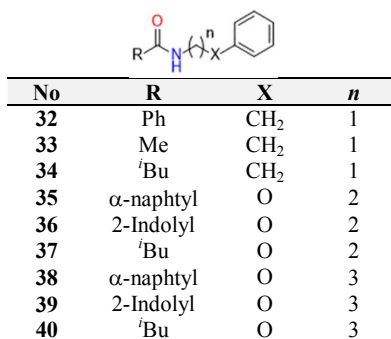


Table 2. The structures of three compounds with the important *ortho* / *para* chlorine substitution on the benzamide moiety.

Synthetic chemistry

In order to expand the preliminary SAR further nine more analogues were synthesised of hit compound **14** (Scheme 2). Three features were deemed important to investigate: First, the tolerance of the benzamide phenyl moiety for substitution with other functional groups;

secondly the length of the alkyl chain and thirdly the tolerance of oxygen substitution in the alkyl chain.



Scheme 2. The nine analogues of hit compound **14** synthesised for SAR generation.

Biological testing revealed that only compound **38** showed activity, giving increased p62 and decreased LC3-II expression. This was verified with a dose response experiment. The efficacy of ligand **38** demonstrates that the substitution of the benzamide phenyl moiety with α -naphthyl is possible and that introduction of an ether link into the alkyl chain is also tolerated. The length of the linker chain is clearly important, with four units optimal, as seen for both hit compound **14** and its derivative **38** compared to ligands **32-37**, which have a shorter chain length. Even though twenty five compounds were tested in this preliminary analysis, a clear SAR was not evident. Thus, substantially more analogues of the hit compounds need to be tested in order to produce a full SAR.

Main screen

For the main screen, the complete diversity ChemBridge diversity collection was used consisting of 5×10^4 molecules.¹² After making it Lipinski compliant 4.3×10^4 entities remained. All four scoring functions available in the GOLD software suite (GoldScore,¹⁴ ChemScore,^{14, 15} ChemPLP²⁰ and ASP²¹) were used in conjunction with the consensus concept, i.e., only ligands that scored well with all the functions and showed hydrogen

bonding activity were taken forward.^{22, 23} For the initial screen it sufficed to take only compounds with good hydrogen bonding ($HB \geq 1$) forward resulting in 1470 candidates. For the second screen, using higher search efficiency and more docking runs, again only ligands with good hydrogen bonding were taken forward as well as a good score (GoldFitness ≥ 45 , ChemSocre ≥ 20 , PLPScore ≥ 50 and ASP ≥ 25) leaving 200 candidates. These were visually inspected using the same criteria as for the pilot screen. Twenty-two ligands were selected for experimental testing and their structures are shown in Table 3.

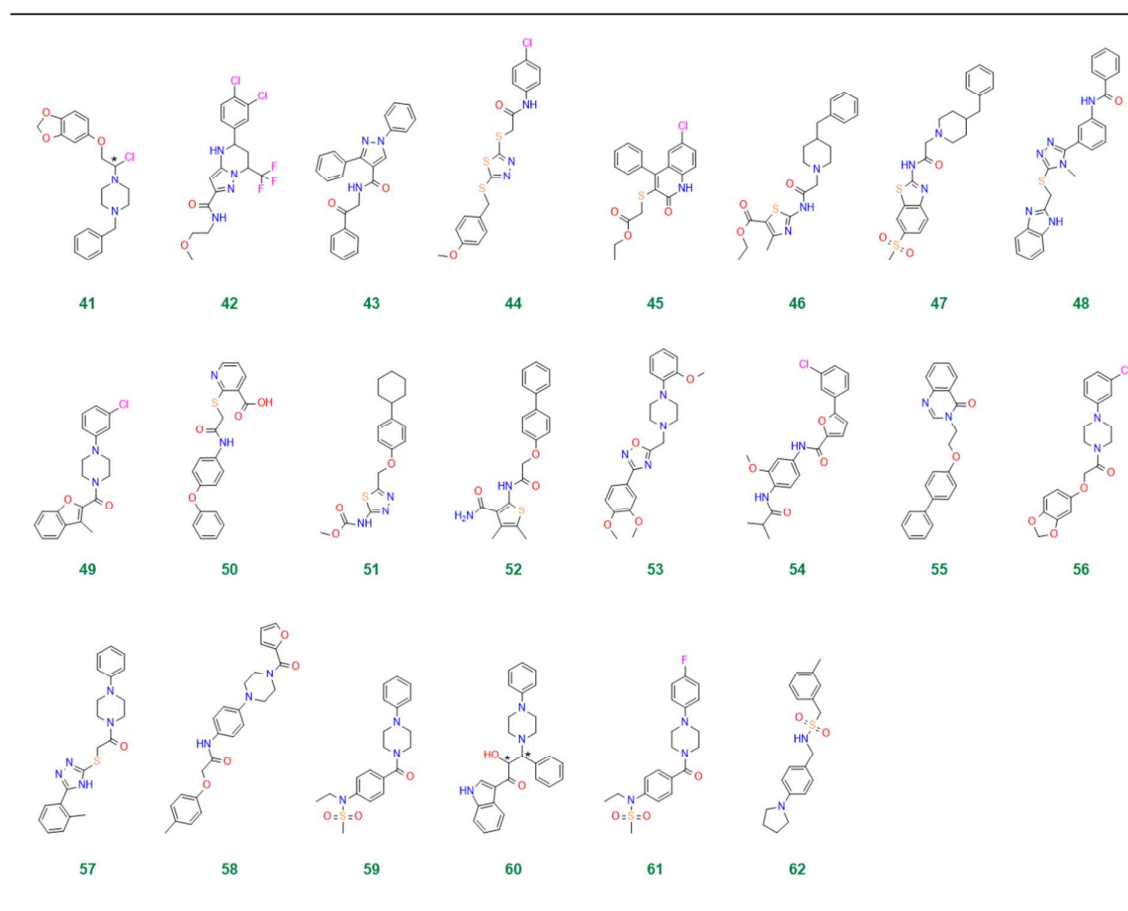


Table 3. The structures of the twenty-two compounds tested for autophagy effect identified from the main virtual screen. Compound **41** and **60** were tested as the racemates.

From the twenty-two virtual hits tested in the ovarian cancer cells ligand **62** caused an increase in p62 and decrease in LC3-II consistent with inhibition of autophagy (see Figure S4). This was also seen for ligand **58** to some extent but the effect was less pronounced than for **62**.

Hit verification

In order to verify the activity of the three hit compounds **14**, **38** and **62** in blocking autophagy cells back to the normal state they were tested in the MCF-7 human breast cancer cell line.

The results are shown in Figure 4.

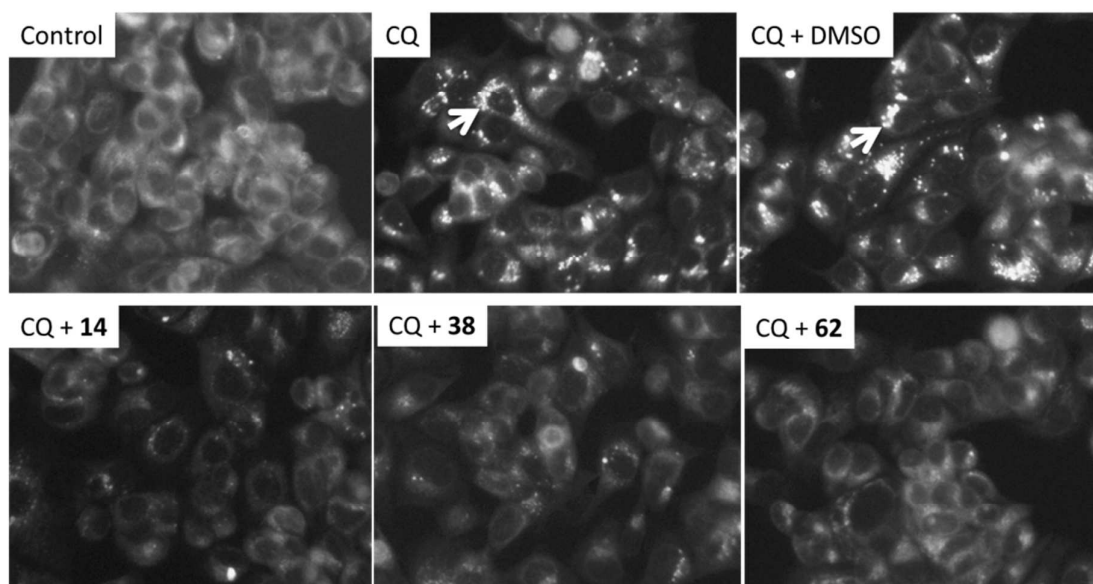


Figure 4. The effect of pre-treating MCF-7 human breast cancer cells with hit compounds **14**, **38** and **62** before incubation with 75 μ M chloroquine (CQ). Autophagolysosomes were visualized by monodansylcadaverine (MDC) staining (see arrows). MDC was loaded into cells and incubated at 37°C for 10 min and visualized by fluorescent microscopy. The pre-incubation with the hit compounds abrogated the CQ induced autophagolysosomes accumulation.

Chloroquine (CQ) is a lysosomotropic agent that prevents autophagy protein degradation by inhibiting lysosome-mediated proteolysis and causes autophagolysosomes accumulation.²⁴

The auto-fluorescent compound monodansylcadaverine (MDC) is a widely used marker of autophagolysosomes as it labels vacuoles formation in later stages in the autophagy

degradation process.²⁵⁻²⁷ Incubation of cells with 75 μM CQ caused a significant increase in the number of autophagolysosomes, visualized by MDC accumulation in vacuoles (Figure 4). The administration of the hits, **14**, **38** and **62**, resulted in effective suppression of the autophagolysosome formation in line with the hypothesis of Atg5-Atg16 complex inhibition. Finally, hit **62** was tested in the well-established National Cancer Institute's NCI60 panel of 60 human tumour cells lines.²⁸ It had a marginal effect on the growth of the cell lines with a mean of 90.1% at 10 μM as compared to 100% of untreated cells. These data suggest that the effect of compound **62** was not dependent on inhibition of cell growth. The result from the NCI60 experiment is shown in Figure S5 in the Supplementary Information.

Modelling of hit compounds

The binding to Atg5 of the three hit compounds was investigated. The predicted binding modes of hit **14** are shown in Figure 5.

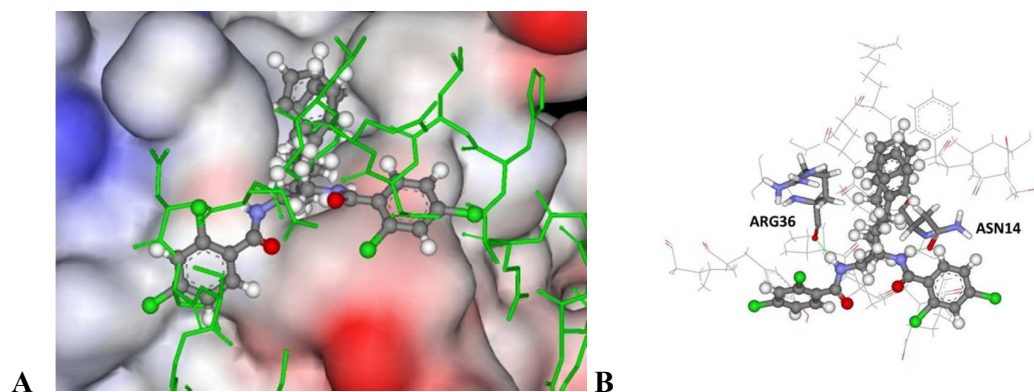


Figure 5. The docked configuration of **14** in the binding site of Atg5 using GoldScore and ChemScore. (A) The protein surface is rendered. The phenyl group of **14** occupies a lipophilic cleft overlapping with the Phe46 amino acid in Atg16, which is shown as green sticks. Red depicts a positive partial charge on the surface, blue depicts negative partial charge and grey shows neutral/lipophilic areas. (B) Hydrogen bonds are shown as green lines between ligand **14** and the amino acids Arg36 for the GoldScore results and Asn14 for the ChemScore configuration.

The modelling of **14** resulted in two plausible binding modes to Atg5. GoldScore and ChemPLP predict the same conformation with hydrogen bonding to the backbone carboxylic moiety of Arg36 but ChemScore predicts bonding to the backbone carboxylic moiety of

Asn14 (Fig. 5B). In both cases the phenyl moiety of **14** occupies the lipophilic cleft in place of Phe46 of the Atg16 polypeptide and overlaps with it in general (Fig. 5A). The ASP scoring function produced a different binding mode to its counterparts but the lipophilic cleft was also occupied by the phenyl moiety. Hit compounds **38** and **62** gave less consistent results when modelled but in all cases the lipophilic binding cleft was filled, suggesting that this may be necessary for the efficacy of the compounds.

Discussion

It is becoming more apparent that the autophagy process plays a pivotal role in diseases such as cancer, *e.g.*, apoptotic cancer cells induced by chemotherapeutics can not only survive but recover from damage with the aid of heightened autophagy activity.²⁹ The implication is that inhibiting autophagy with small molecules may increase the efficacy of chemotherapeutic regimes.

The three hits found in this project are a good start in developing effective inhibitors for autophagy. At this stage, we cannot rule out the possibility that the compounds inhibit autophagy through some mechanism other than interfering with Atg5-atg16 complex formation. The development of a specific biochemical assay, isothermal calorimetric titration (ICT) experiments and/or X-ray crystallography will answer this vital question. In particular, the results of ICT experiments can reveal whether the hits can perturb the Atg5-Atg16 complex formation and we are currently evaluating this. Furthermore, the exploration of chemical space surrounding the hits by chemical synthesis will produce a more complete SAR, identifying more potent ligands and aiding in developing a better molecular model. The SAR study presented here can only be viewed as preliminary. Nevertheless, having the three hit compounds identified in this work is the crucial start to give traction to develop

autophagy-specific inhibitors and hopefully leading to an effective adjunctive therapeutic approach in the treatment of cancer.

Conclusion

In this work two hit compounds **14** and **62** were identified using virtual high throughput screening inhibiting autophagy in ovarian A2780 cancer cells. Preliminary SAR was developed for hit **14** leading to the discovery of another active compound **38**. The three active compounds were tested in MCF-7 breast cancer cells and the characteristic autophagy vacuole formation was diminished upon the administration of the inhibitors verifying their efficacy. These three compounds can now be developed further with more elaborate experimental / biological testing and by substantially extending the SAR analysis.

Methodology

Modelling and screening

The compounds were docked to the crystal structure of Atg16–Atg5 (PDB ID: 2DYO, resolution 1.97 Å),⁶ which was obtained from the Protein Data Bank (PDB).^{30, 31} The Scigress Ultra version 7.7.0.47 program³² was used to prepare the crystal structure for docking, i.e., hydrogen atoms were added, the co-crystallised polypeptide Atg-16 was removed as well as crystallographic water molecules. The centre of the binding pocket was defined as the position of the Atg-16's Phe-46 of the *para*-carbon of the phenyl ring ($x = 87.120$, $y = 88.114$, $z = 69.571$) with 10 Å radius. For the initial screen 30% search efficiency was used (virtual screen) with ten runs per compound. For the second phase (re-dock) 100% efficiency was used in conjunction with fifty docking runs. The GoldScore (GS),¹⁴ ChemScore (CS),^{15, 16} ChemPLP²⁰ and ASP²¹ scoring functions were implemented to validate the predicted binding modes and relative energies of the ligands using the GOLD v5.2 software suite. The virtual

high throughput screen was conducted with the ChemBridge diversity collection of 5×10^4 entities.¹² Substructure and Tanimoto similarity search methods³³ were used to identify the structurally related compounds using the Hit2Lead¹² web based compound libraries.

Western blotting

The investigational compounds identified through screening for autophagic activity were used in cell-based assays to determine their effects on autophagy in ovarian cancer cells. A2780 cells (5×10^5 cells/well) were plated in 6-well plates in 1 mL of growth medium and pre-incubated for 24 h. Following this, the cells were incubated with 50-100 μM of each compound for 1 h before replacing the medium in each well with PBS supplemented with the corresponding compound. DMSO was added to the control wells to equal the concentration in drug-treated wells (max. 0.5%). After 3 h of PBS-induced autophagy, cells were lysed and autophagy-specific proteins detected and autophagy-specific proteins (LC3-II and p62) detected using western blotting with GAPDH used as loading control. Each compound was tested in two or three independent experiments. Further dose-response assays were performed with investigational compounds that demonstrated autophagy inhibition in the initial assay. Similar assays were performed with four concentrations (12.5 μM , 25 μM , 50 μM and 100 μM) of each compound. The concentration of DMSO was normalised across all wells for each experiment.

The buffer used for A2780 ovarian cancer cells lysis was prepared consisting of 20 mM HEPES, 150 mM NaCl, 2 mM EDTA, 0.5% sodium deoxycholate, 1% NP40, 120 μM leupeptin, 1 μM pepstatin and 1 mM PMSF. The concentration of protein within the lysate was established using Sigma supplied bicinchoninic acid kit. Nusep 4-20% polyacrylamide gradient gel was used, loading between 5-15 μg protein per sample. After protein separation on gel, the proteins were transferred onto the PVDF membrane, which was then blocked in 5% skimmed milk powder dissolved in TBST buffer consisting of 50 mM Tris-HCl, pH 7.4,

150 mM NaCl, 0.1% Tween 20, for 1 h at RTP. The membrane was then incubated in antibodies for ~16 h (overnight) at temperature of 4°C, where LC3-2G6 (Nanotools) at 1/2000 dilution was utilised as anti-LC3 antibody and AB56416 (Abcam) at 1/1000 dilution was used as anti-SQSTM1/p62 antibody. The dilution step was then repeated in 5% milk in TBST as above, and subsequently in anti-GAPDH antibody MAB374 (Millipore) at 1/5000 dilution for 1 h at RTP. After each primary antibody, the membrane was washed three times for 5 min. The membrane was then incubated in anti-mouse IgG antibody linked to HRP (Cell Signalling Technology) at 1/2000 dilution in a room temperature for a period of 1 h. Membrane was then washed in TBST five times consecutively, before the detection of protein bands, which was conducted using UptiLight HRP chemiluminescent substrate (Uptima) and a FluorChem M Imager. To quantitate individual proteins, signal intensity was integrated over the area of each band and corrected for background. Results were normalized to GAPDH measured in the same sample.

MCF-7 breast cancer cells

Human breast cancer cell line MCF-7 grown in 96 well plates were not treated (control) or treated with chloroquin (75µM) alone or with **14**, **38** and **62** at 25 µM. DMSO (0.2%) was incubated for vehicle control. After 5 hours, cells were incubated with 10 µM monodansylcadaverine (MDC, Sigma, 30432) for 20 min at 37°C, then washed with PBS three times. Images were examined immediately by fluorescence microscopy (FLoid Cell Imaging Station, 40 × magnification).

NCI's 60-cell line panel growth inhibition assay

The compounds obtained were submitted to the National Cancer Institute's Developmental Therapeutic Program (DTP) where they were screened against a panel of sixty human tumour

cell lines (NCI60,²⁸ for further information see ref. and references therein). The full description of the assay is given in the Supplementary Information.

Chemistry

Known compounds **32-34** were prepared by acylation of phenethylamine hydrochloride using standard conditions. Experimental procedures and characterisation data are provided in the Supporting Information. Compounds **35-40** were prepared from either 2- or 3-phenoxyethylamine, as described below.

2-Phenoxyethylamine: A solution of 2-iodo-*N*-Boc-ethylamine (313 mg, 1.2 mmol), phenol (163 mg, 1.7 mmol, 1.5 equiv.) and potassium carbonate (280 mg, 2.0 mmol, 1.8 equiv.) in dimethylformamide (3 mL) was stirred at room temperature for 24 hours before being poured into ether (25 mL). The organic phase was washed with water, 2M NaOH and brine (15 mL), dried over anhydrous magnesium sulfate, filtered and concentrated *in vacuo*. The crude oil (226 mg, 0.95 mmol) was dissolved in dichloromethane (1.5 mL) and trifluoroacetic acid (250 μ L, 3.3 mmol, 3.4 eq) added. The reaction mixture was stirred at room temperature for 18 h then poured into a mixture of ethyl acetate and 1M NaOH (1:1, 20 mL). The aqueous phase was extracted with further ethyl acetate (10 mL) and the combined organic phases washed with brine (10 mL), dried over anhydrous magnesium sulfate, filtered and concentrated *in vacuo* to give as a brown oil (130 mg) that was used without further purification.

3-Phenoxypropylamine: Prepared according to the procedure for 2-phenoxyethylamine above, beginning from 3-iodo-*N*-Boc-propylamine (328 mg, 1.2 mmol) to give crude

3-phenoxypropylamine (216 mg) as a colourless oil that was used without further purification.

N-(2-phenoxyethyl)-1-naphthamide (**35**): To a solution of 1-naphthoic acid (163 mg, 0.95 mmol) in dichloromethane-dimethylformamide (3:1, 4 mL) were added DCC (206 mg, 1.00 mmol, 1.05 equiv.) and 6-Cl-HOBt (32 mg, 0.19 mmol, 0.20 equiv.) and the mixture stirred at room temperature for 30 min. A solution of crude 2-phenoxyethylamine (130 mg, 0.95 mmol, 1.0 equiv.) in dichloromethane (2 mL) was added over 15 min and the mixture stirred at rt for 18 h. The reaction mixture was then filtered and the combined filtrate and washings (EtOAc) washed with 1M HCl, 1M NaOH and brine, dried over anhydrous magnesium sulfate, filtered and concentrated *in vacuo*. Column chromatography (EtOAc-hexanes) afforded **35** (126 mg, 38%) as a colourless solid. ¹H NMR (400 MHz, CDCl₃): 8.34 (1H, m), 7.91 (1H, d, *J* = 8 Hz), 7.86 (1H, m), 7.61 (1H, dd, *J* = 7, 0.8 Hz), 7.56-7.49 (2H, m), 7.45 (1H, dd, *J* = 8, 7 Hz), 7.30 (2H, dd, *J* = 8, 7 Hz), 6.98 (1H, t, *J* = 7 Hz), 6.93 (2H, d, *J* = 8 Hz), 6.52 (1H, bs), 4.22 (2H, t, *J* = 5 Hz), 3.95 (2H, q, *J* = 6 Hz); ¹³C NMR (100 MHz, CDCl₃): 169.8, 158.6, 134.4, 133.8, 130.9, 130.2, 129.7, 128.5, 127.3, 126.6, 125.5, 125.3, 124.9, 121.4, 114.6, 66.8, 39.7; IR: 3413, 3274, 3053, 2935, 2876, 1641, 1597, 1527, 1496, 1463, 1436, 1392, 1244 cm⁻¹; HRMS(ESI) *m/z* calcd for C₁₉H₁₇NNaO₂ [M+Na]⁺: 314.1151, found: 314.1147; TLC: R_f 0.27 (40% EtOAc-hexanes).

N-(2-phenoxyethyl)-1*H*-indole-2-carboxamide (**36**): Prepared according to the method described for **35** above, from indole-2-carboxylic acid (153 mg, 0.95 mmol, 1.00 equiv.) and 2-phenoxyethylamine (130 mg, 0.95 mmol, 1.0 equiv.). The crude oil was purified by recrystallization (hexane-EtOAc, reflux) to afford **36** (125 mg, 39%) as brown crystals. ¹H NMR (400 MHz, *d*₆-DMSO): 8.70 (1H, t, *J* = 6 Hz), 7.61 (1H, dd, *J* = 8, 1 Hz), 7.43 (1H, dd,

$J = 8, 1 \text{ Hz}$), 7.32-7.25 (2H, m), 7.17 (1H, ddd, $J = 8, 7, 1 \text{ Hz}$), 7.14 (1H, dd, $J = 2, 1 \text{ Hz}$), 7.03 (1H, ddd, $J = 8, 7, 1 \text{ Hz}$), 7.00- 6.96 (2H, m), 6.93 (1H, tt, $J = 7, 1 \text{ Hz}$), 4.13 (2H, t, $J = 6 \text{ Hz}$), 3.67 (2H, q, $J = 6 \text{ Hz}$); ^{13}C NMR (100 MHz, d_6 -DMSO): 161.4, 158.4, 136.4, 131.5, 129.5, 127.1, 123.3, 121.5, 120.7, 119.7, 114.5, 112.3, 102.6, 66.0, 38.5; IR: 3401, 3287, 2927, 2852, 1625, 1600, 1548, 1496, 1465, 1418, 1384, 1341, 1309, 1248 cm^{-1} HRMS(ESI) m/z calcd for $\text{C}_{17}\text{H}_{16}\text{N}_2\text{NaO}_2$ $[\text{M}+\text{Na}]^+$: 303.1104, found: 303.1100; TLC: R_f 0.27 (40% EtOAc-hexane).

3-Methyl-N-(2-phenoxyethyl)butanamide (**37**): To a solution of 2-phenoxyethylamine (216 mg, 1.4 mmol) and triethylamine (350 μL , 2.5 mmol, 1.8 equiv.) in dichloromethane (6 mL) at 0 $^\circ\text{C}$ under nitrogen was added isovaleryl chloride (250 μL , 2.1 mmol, 1.44 equiv.) dropwise over 5 min. The reaction mixture was stirred at room temperature for 24 h then poured into ethyl acetate (10 mL) and the organic phase washed with 1M HCl and 1M NaOH. The aqueous phases were further extracted with ethyl acetate and the organic phase washed with 1M HCl and 1M NaOH. The combined organic phases were then washed with brine, dried over anhydrous magnesium sulfate, filtered and concentrated *in vacuo* to give a light brown oil. Column chromatography (EtOAc-hexanes, 1:1–2:1) afforded **37** (95 mg, 35%) as an off-white solid. ^1H NMR (400 MHz, CDCl_3): 7.29 (2H, tm, $J = 8.0 \text{ Hz}$), 6.97 (1H, tm, $J = 8.0 \text{ Hz}$), 6.89 (2H, dm, $J = 8 \text{ Hz}$), 5.89 (1H, bs), 4.04 (2H, t, $J = 5 \text{ Hz}$), 3.67 (2H, q, $J = 6 \text{ Hz}$), 2.17-2.05 (3H, m), 0.95 (6H, d, $J = 6 \text{ Hz}$); ^{13}C NMR (100 MHz, CDCl_3): 172.8, 158.6, 129.7, 121.3, 114.6, 67.0, 46.3, 39.0, 26.3, 22.6; IR (cm^{-1}) 3290, 3073, 2956, 2931, 2871, 1643, 1600, 1588, 1545, 1496, 1464, 1387, 1368, 1300, 1243, 1216 cm^{-1} ; HRMS: (ESI) m/z calcd for $\text{C}_{13}\text{H}_{19}\text{NNaO}_2$ $[\text{M}+\text{Na}]^+$ 244.1308, found 244.1315; R_f 0.27 (EtOAc-hexanes, 1:1).

N-(3-Phenoxypropyl)-1-naphthamide (**38**): Prepared according to the method described for **35** above, from 1-naphthoic acid (254 mg, 1.48 mmol, 1.03 equiv.) and 3-phenoxyethylamine (216 mg, 1.43 mmol, 1.0 equiv.). The crude oil was purified by chromatography (EtOAc-hexane, 2:1) to yield **38** (161 mg, 46 %) as a colourless solid. ^1H NMR (400 MHz, CDCl_3): 8.33 (1H, m), 7.91 (1H, d, $J = 8$ Hz), 7.87 (1H, m), 7.59 (1H, dd, $J = 7, 1$ Hz), 7.52 (2H, m), 7.44 (1H, dd, $J = 8, 7$ Hz), 7.27 (2H, m), 6.95 (1H, tt, $J = 7, 1$ Hz), 6.85 (2H, dm, $J = 8$ Hz), 6.47 (1H, bs), 4.15 (2H, t, $J = 6$ Hz), 3.77 (2H, q, $J = 6$ Hz), 2.18 (2H, quintet, $J = 6$ Hz); ^{13}C NMR (100 MHz, CDCl_3): 169.6, 158.5, 134.7, 133.8, 130.6, 130.2, 129.6, 128.3, 127.1, 126.4, 125.5, 124.9, 124.7, 121.1, 114.4, 66.5, 38.2, 29.1; IR: 3413, 3279, 3056, 2939, 2876, 1639, 1592, 1534, 1497, 1471, 1434, 1393, 1300, 1243, 1215 cm^{-1} HRMS(ESI) m/z calcd for $\text{C}_{20}\text{H}_{19}\text{NNaO}_2$ $[\text{M}+\text{Na}]^+$: 328.1308, found: 328.1299; TLC: R_f 0.29 (40% EtOAc-hexane).

N-(3-phenoxypropyl)-1H-indole-2-carboxamide (**39**): Prepared according to the method described for **35** above, from indole-2-carboxylic acid (250 mg, 1.55 mmol, 1.08 equiv.) and 3-phenoxyethylamine (216 mg, 1.43 mmol, 1.0 equiv.). The crude oil was purified by chromatography (EtOAc-hexane, 2:1) to yield **39** (189 mg, 46 %) as a flaky, off-white solid. ^1H NMR (400 MHz, CDCl_3): 11.55 (1H, s), 8.55 (1H, t, $J = 6$ Hz), 7.60 (1H, dd, $J = 8, 0.6$ Hz), 7.42 (1H, dd, $J = 8, 1$ Hz), 7.28 (2H, m), 7.17 (1H, ddd, $J = 8, 7, 1$ Hz), 7.11 (1H, dd, $J = 2, 1$ Hz), 7.02 (1H, ddd, $J = 8, 7, 1$ Hz), 6.96-6.89 (3H, m), 4.05 (2H, t, $J = 6$ Hz), 3.46 (2H, q, $J = 6$ Hz), 2.01 (2H, quint., $J = 6$ Hz); ^{13}C NMR (100 MHz, CDCl_3): 161.2, 158.6, 136.4, 131.8, 129.5, 127.1, 123.2, 121.4, 120.5, 119.6, 114.4, 112.3, 102.3, 65.1, 35.9, 29.1; IR: 3244, 3075, 3056, 2989, 2944, 1609, 1563, 1497, 1471, 1425, 1418, 1383, 1368, 1341, 1317, 1307, 1271, 1240, 1213 cm^{-1} ; HRMS(ESI) m/z calcd for $\text{C}_{20}\text{H}_{19}\text{NNaO}_2$ $[\text{M}+\text{Na}]^+$: 317.1260, found: 317.1253; TLC: R_f 0.29 (40% EtOAc-hexane).

3-Methyl-N-(2-phenoxyethyl)butanamide (40): Prepared according to the method described for **37** above, from 3-phenoxyethylamine (216 mg, 1.43 mmol, 1.0 equiv.) and isovaleryl chloride (250 μ L, 2.06 mmol, 1.44 equiv.). The crude product was purified by chromatography (EtOAc-hexane, 1:1-2:1) to yield **40** (95 mg, 35 %) as a flaky, off-white solid. ^1H NMR (400 MHz, CDCl_3): 7.29 (2H, m), 6.96 (1H, tm, $J = 8$ Hz), 6.89 (2H, dm, $J = 8$ Hz), 5.82 (1H, bs), 4.04 (2H, t, $J = 6$ Hz), 3.47 (2H, q, $J = 6$ Hz), 2.11 (1H, m), 2.05 – 1.95 (4H, m), 0.95 (6H, d, $J = 6$ Hz); ^{13}C NMR (100 MHz, CDCl_3): 172.7, 158.7, 129.7, 121.1, 114.6, 66.4, 46.4, 37.5, 29.2, 26.3, 22.6; IR: 3299, 3069, 2956, 2927, 2871, 1632, 1600, 1589, 1547, 1499, 1473, 1451, 1384, 1364, 1303, 1292, 1249 cm^{-1} ; HRMS(ESI) m/z calcd for $\text{C}_{14}\text{H}_{21}\text{NNaO}_2$ $[\text{M}+\text{Na}]^+$: 258.1465, found: 258.1464; TLC: R_f 0.24 (hexane- EtOAc, 1 : 1).

Acknowledgements

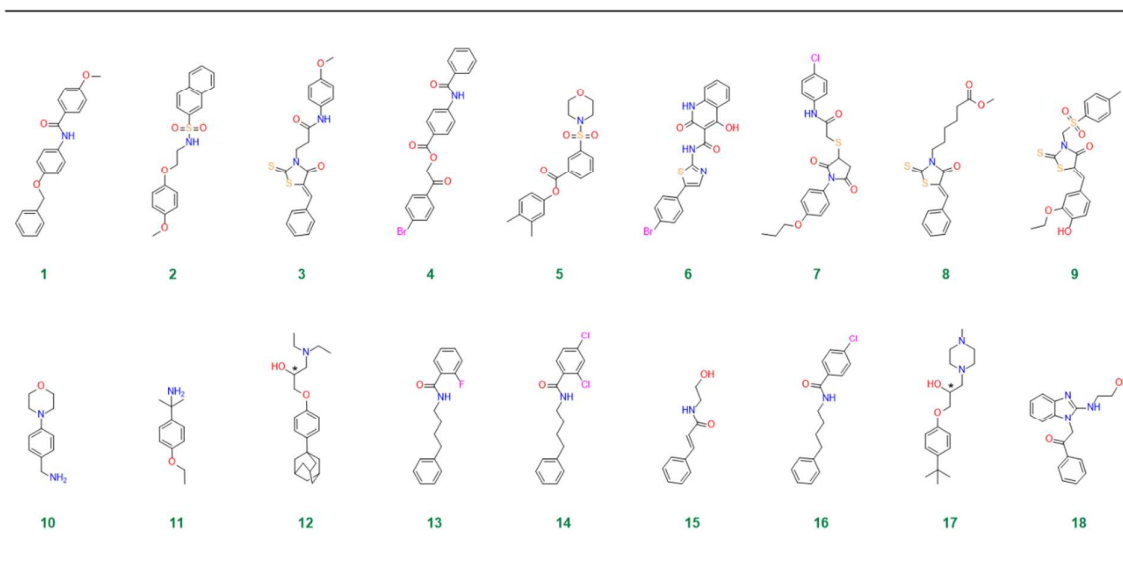
Funding for this work was obtained from the Maurice and Phyllis Paykel trust, the McClelland Trust, Auckland Medical Research Foundation and Genesis Oncology Trust (GOT-1429-PDA). This work is also supported by Auckland Cancer Society Research Centre.

References

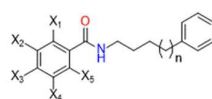
- 1 A. Kaufmann, V. Beier, H. G. Franquelim and T. Wollert, *Cell*, 2014, **156**, 469–481.
- 2 N. N. Noda, Y. Ohsumi and F. Inagaki, *Chem. Rev.*, 2009, **109**, 1587-1598.
- 3 E. Morselli, L. Galluzzi, O. Kepp, J.-M. Vicencio, A. Criollo, M. C. Maiuri and G. Kroemer, *Biochim. Biophys. Acta*, 2009, **1793**, 1524-1532.
- 4 N. B. Nedelsky, P. K. Todd and J. P. Taylor, *Biochim. Biophys. Acta*, 2008, **1782**, 691-699.
- 5 A. Fleming, T. Noda, T. Yoshimori and D. C. Rubinsztein, *Nature Chem. Biol.*, 2011, **7**, 9-17.
- 6 M. Matsushita, N. N. Suzuki, K. Obara, Y. Fujioka, Y. Ohsumi and F. Inagaki, *J. Biol. Chem.*, 2007, **282**, 6763-6772.
- 7 Y. Fujioka, N. N. Noda, H. Nakatogawa, Y. Ohsumi and F. Inagaki, *J. Biol. Chem.*, 2010, **285**, 1508-1515.
- 8 A. Brennand, M. Gualdrón-López, I. Coppens, D. J. Rigden, M. L. Ginger and P. A. M. Michels, *Mol. Biochem. Para*, 2011, **177**, 83-99.

- 9 R. V. Guido, G. Oliva and A. D. Andricopulo, *Curr. Med. Chem.*, 2008, **15**, 37-46.
- 10 T. Zhu, S. Cao, P. C. Su, R. Patel, D. Shah, H. B. Chokshi, R. Szukala, M. E. Johnson and K. E. Hevener, *J. Med. Chem.*, 2013, **12**, 6560-6572.
- 11 T. Scior, A. Bender, G. Tresadern, J. L. Medina-Franco, K. Martínez-Mayorga, T. Langer, K. Cuanalo-Contreras and D. K. Agrafiotis, *J. Chem. Inf. Model.*, 2012, **52**, 867-881.
- 12 Hit2Lead <http://www.hit2lead.com/>, in *Hit2Lead* <http://www.hit2lead.com/>, ChemBridge Corporation, 2012, vol. 2011.
- 13 C. A. Lipinski, F. Lombardo, B. W. Dominy and P. J. Feeney, *Adv. Drug Deliv. Rev.*, 1997, **23**, 3-25.
- 14 G. Jones, P. Willet, R. C. Glen, A. R. Leach and R. Taylor, *J. Mol. Biol.*, 1997, **267**, 727-748.
- 15 M. D. Eldridge, C. Murray, T. R. Auton, G. V. Paolini and P. M. Mee, *J. Comp. Aid. Mol. Design*, 1997, **11**, 425-445.
- 16 M. L. Verdonk, J. C. Cole, M. J. Hartshorn, C. W. Murray and R. D. Taylor, *Proteins*, 2003, **52**, 609-623.
- 17 P. Axerio-Cilies, I. P. Castañeda, A. Mirza and J. Reynisson, *Eur. J. Med. Chem.*, 2009, **44**, 1128-1134.
- 18 J. Reynisson, W. Court, C. O'Neill, J. Day, L. Patterson, E. McDonald, P. Workman, M. Katan and S. A. Eccles, *Bioorg. Med. Chem.*, 2009, **17**, 3169-3176.
- 19 K. B. Larsen, T. Lamark, A. Øvervatn, I. Harneshaug, T. Johansen and G. Bjørkøy, *Autophagy*, 2010, **6**, 784-793.
- 20 O. Korb, T. Stütze and T. E. Exner, *J. Chem. Inf. Model.*, 2009, **49**, 84-96.
- 21 W. T. M. Mooij and M. L. Verdonk, *Proteins*, 2005, **61**, 272-287.
- 22 R. Wang and S. Wang, *J. Chem. Inf. Comput. Sci.*, 2001, **41**, 1422-1426.
- 23 J. M. Yang, Y. F. Chen, T. W. Shen, B. S. Kristal and D. F. Hsu, *J. Chem. Inf. Model.*, 2005, **45**, 1134-1146.
- 24 K. A., H. Uchiyama, S. Takano, N. Nakamura and S. Ohkuma, *Autophagy*, 2007, **3**, 154-157.
- 25 D. J. Klionsky, F. C. Abdalla, H. Abeliovich, R. T. Abraham, A. Acevedo-Aroza, K. Adeli, et al., *Autophagy*, 2012, **8**, 445-544.
- 26 E. T. Bampton, C. G. Goemans, D. Niranjana, N. Mizushima and A. M. Tolkovsky, *Autophagy*, 2005, **1**, 23-36.
- 27 K. Vanderlaag, Y. Su, A. E. Frankel, R. C. Burghardt, R. Barhoumi, G. Chadalapaka, I. Jutooru and S. S., *BMC Cancer* 2010, **10**, 669.
- 28 R. H. Shoemaker, *Nat. Rev. Drug Dis.*, 2006, **6**, 813-823.
- 29 J. Thorburn, Z. Andrysik, L. Staskiewicz, J. Gump, P. Maycotte, A. Oberst, D. R. Green, J. M. Espinosa and A. Thorburn, *Cell Rep.*, 2014, **7**, 45-52.
- 30 H. M. Berman, J. Westbrook, Z. Feng, G. Gilliland, T. N. Bhat, H. Weissig, I. N. Shindyalov and P. E. Bourne, *Nuc. Acids Res.*, 2000, **28**, 235-242.
- 31 H. Berman, K. Henrick and H. Nakamura, *Nat. Struct. Biol.*, 2003, **10**, 980.
- 32 Scigress Explorer Ultra Version 7.7.0.47, Fujitsu Limited, 2000 - 2007.
- 33 A. R. Leach and V. J. Gillet, 1. Representation and manipulation of 2D molecular structures, in *An Introduction to Chemoinformatics*, Kluwer Academic Publisher, Dordrecht, 2003, pp. 1-26.

Table 1

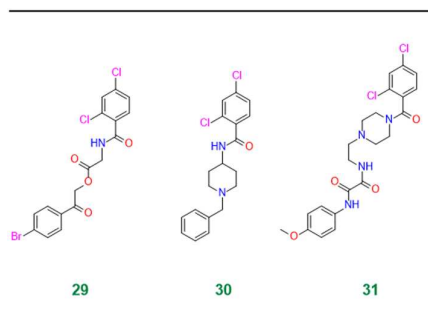


Scheme 1:

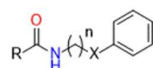


- 13: $X_1 = F, n = 1$
 14: $X_1 = Cl, X_3 = Cl, n = 1$
 16: $X_3 = Cl, n = 1$
 19: $X_1 = Cl, X_4 = Cl, n = 1$
 20: $X_2 = F, n = 1$
 21: $X_1 = Cl, X_5 = Cl, n = 1$
 22: $X_1 = Br, n = 1$
 23: $X_2 = Br, n = 1$
 24: $X_3 = Br, n = 1$
 25: $X_1 = Cl, n = 1$
 26: $X_3 = F, n = 1$
 27: $X_2 = Cl, X_3 = Cl, n = 1$
 28: $n = 0$

Table 2:



Scheme 2:



No	R	X	n
32	Ph	CH ₂	1
33	Me	CH ₂	1
34	^t Bu	CH ₂	1
35	α-naphtyl	O	2
36	2-Indolyl	O	2
37	^t Bu	O	2
38	α-naphtyl	O	3
39	2-Indolyl	O	3
40	^t Bu	O	3

Table 3:

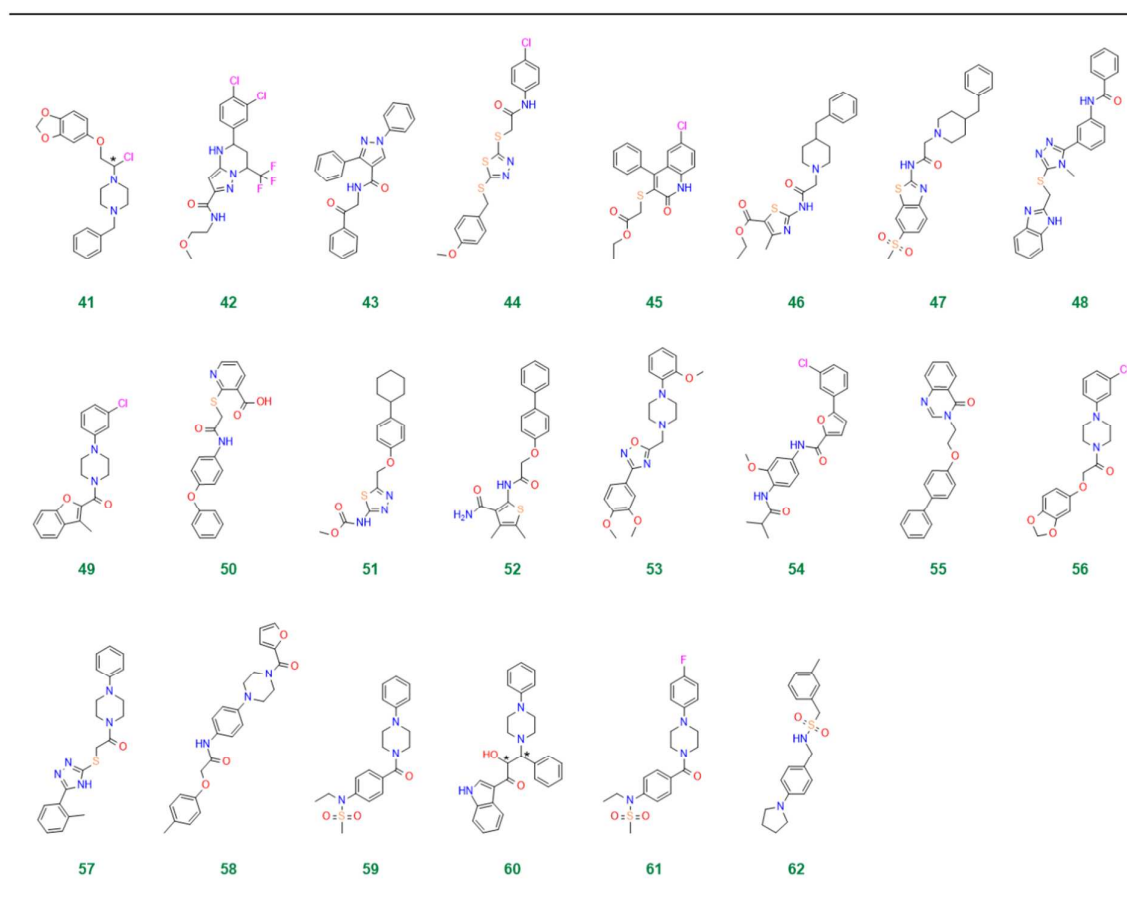
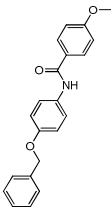
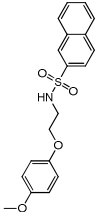
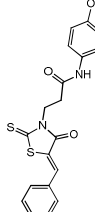
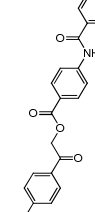
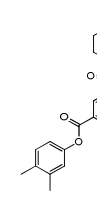
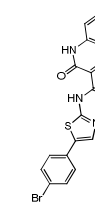

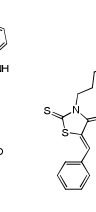

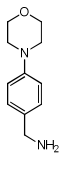
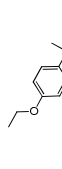
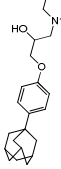

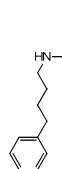
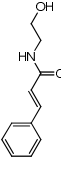
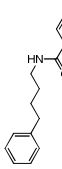
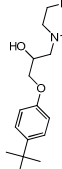
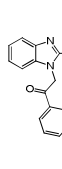
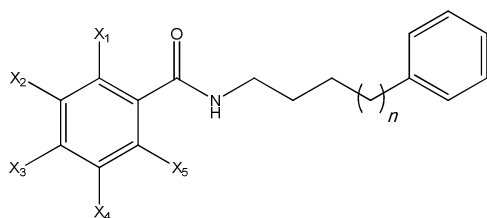


Table 1

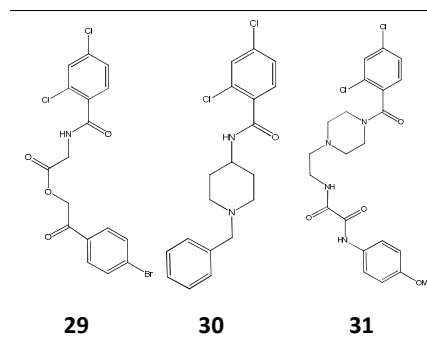
								
1	2	3	4	5	6	7	8	9
								
10	11	12	13	14	15	16	17	18

Scheme 1



- 13** $X_1 = F, n = 1$
14 $X_1 = Cl, X_3 = Cl, n = 1$
16 $X_3 = Cl, n = 1$
19 $X_1 = Cl, X_4 = Cl, n = 1$
20 $X_2 = Cl, n = 1$
21 $X_1 = Cl, X_5 = Cl, n = 1$
22 $X_1 = Br, n = 1$
23 $X_2 = Br, n = 1$
24 $X_3 = Br, n = 1$
25 $X_1 = Cl, n = 1$
26 $X_3 = F, n = 1$
27 $X_2 = Cl, X_3 = Cl, n = 1$
28 $n = 0$

Table 2



Scheme 2

**32** R = Ph**33** R = Me**34** R = *i*Bu**35** R = α -naphthyl $n = 1$ **36** R = 2-indolyl 1**37** R = *i*Bu 1**38** R = α -naphthyl $n = 2$ **39** R = 2-indolyl 2**40** R = *i*Bu 2

Table 3

